

Analysis of the phase transition in the two-dimensional Ising ferromagnet using a Lempel-Ziv string-parsing scheme and black-box data-compression utilities

O. Melchert* and A. K. Hartmann†

Institut für Physik, Universität Oldenburg, Carl-von-Ossietzky Strasse, 26111 Oldenburg, Germany

(Received 10 June 2014; published 13 February 2015)

In this work we consider information-theoretic observables to analyze short symbolic sequences, comprising time series that represent the orientation of a single spin in a two-dimensional (2D) Ising ferromagnet on a square lattice of size $L^2 = 128^2$ for different system temperatures T . The latter were chosen from an interval enclosing the critical point T_c of the model. At small temperatures the sequences are thus very regular; at high temperatures they are maximally random. In the vicinity of the critical point, nontrivial, long-range correlations appear. Here we implement estimators for the entropy rate, excess entropy (i.e., “complexity”), and multi-information. First, we implement a Lempel-Ziv string-parsing scheme, providing seemingly elaborate entropy rate and multi-information estimates and an approximate estimator for the excess entropy. Furthermore, we apply easy-to-use black-box data-compression utilities, providing approximate estimators only. For comparison and to yield results for benchmarking purposes, we implement the information-theoretic observables also based on the well-established M -block Shannon entropy, which is more tedious to apply compared to the first two “algorithmic” entropy estimation procedures. To test how well one can exploit the potential of such data-compression techniques, we aim at detecting the critical point of the 2D Ising ferromagnet. Among the above observables, the multi-information, which is known to exhibit an isolated peak at the critical point, is very easy to replicate by means of both efficient algorithmic entropy estimation procedures. Finally, we assess how good the various algorithmic entropy estimates compare to the more conventional block entropy estimates and illustrate a simple modification that yields enhanced results.

DOI: [10.1103/PhysRevE.91.023306](https://doi.org/10.1103/PhysRevE.91.023306)

PACS number(s): 02.70.-c, 75.40.Mg, 05.70.Jk, 89.70.Cf

I. INTRODUCTION

The standard analysis of phase transitions in terms of statistical mechanics involves the analysis of order parameters and other derivatives of the free energy, related to a given model system [1]. Routinely, one studies model systems that involve many degrees of freedom and local interactions that nevertheless result in a nontrivial, seemingly “complex” behavior. Implying a rather naive use of the word, such systems are regarded as being very complex, particularly right at the point where a phase transition occurs in the underlying model. From a point of view of statistical mechanics, a large degree of complexity is shown by growing correlations as one approaches the critical point by tuning a proper system parameter. Correspondingly, throughout the analysis of observables related to such model systems it is often desirable to find a measure for what is naively referred to as the “complexity” of the underlying system [2,3]. However, a precise definition of the term complexity is often elusive. An alternative approach to the analysis of phase transitions, which has recently gained popularity in the analysis of complex systems, is based on a purely information theoretic approach [4–6]. A variety of previous studies employed such information-theoretic methods to measure the entropy rate (i.e., disorder and randomness) and statistical complexity (i.e., structure, patterns and correlations) for $d \geq 1$ -dimensional systems [4,7–12]. In particular for one-dimensional (1D) systems, the excess entropy constitutes a well-understood information-theoretic measure of complexity, providing a well-defined literal sense

for that term. Effectively, the excess entropy accounts for the rapidity of entropy convergence. In order to obtain numerical values for the entropy rate and complexity, the well-established information-theoretic approach presented in Ref. [5] is based on the notion of a “block entropy”; see discussion below. Among several intriguing findings, it led to the analysis of complexity-entropy diagrams that allow for a characterization of the temporal and spatial dynamics of various stochastic processes, including simple maps as well as Ising spin systems, in purely information-theoretic coordinates [4].

On the other hand, note that there are a variety of other measures for what is known as algorithmic entropy, as, e.g., the description size of a minimal algorithm (or computer, or circuit), which is able to generate an instance of the problem under scrutiny [13–15]. However, such measures are often impractical when it comes to the analysis of large systems. In this regard, as discussed in the literature [16,17], particular data-compression algorithms might render a natural and particularly simple candidate for estimating an algorithmic entropy. The pivotal challenge of such data-compression algorithms, readily available as black-box data-compression utilities such as, e.g., the *zlib* [18], *bzip2* [19], and *lzma* [20] utilities, is to discover *patterns* (synonymous with regularities, correlations, symmetries, and structure; see Sec. II of Ref. [21]) in the given input data and to exploit the respective redundancies in order to minimize the space required to store the data. Interestingly, the pattern discovery and data-compression process of particular data-compression schemes finds application in contexts as diverse as, e.g., DNA sequence classification [22], entropy estimation [16,23,24], and, more generally, time series analysis [17]. However, at this point, please note that not all of the applications of such methods reported in the scientific literature are without critique; see [25–27].

*oliver.melchert@uni-oldenburg.de

†alexander.hartmann@uni-oldenburg.de

In this study we aim to assess how well algorithmic entropy (AE) estimates, obtained using a Lempel-Ziv (LZ) string-parsing scheme [28,29] and black-box data-compression utilities, and the results obtained therewith compare to those obtained by means of the respective block entropy (BE) estimates used in the context of the information-theoretic approach mentioned earlier. As raw data, to be processed further by both approaches, we consider binary sequences that represent the spin-flip dynamics, induced by single-spin-flip Metropolis updates [30] of the 2D Ising ferromagnet (FM) on a square lattice of side length $L = 128$ with fully periodic boundary conditions at different temperatures T . The temperatures are chosen from the interval $T \in [2, 2.8]$, enclosing the critical point $T_c = 2.269\dots$ of the model. In order to model the binary sequences, a particular spin on the lattice is chosen as a “source,” emitting symbols from the binary alphabet $\mathcal{A} = \{0, 1\}$ (after a simple transformation of the spin variables). Therefore, the orientation of the source spin is monitored during a number of N Monte Carlo (MC) sweeps to yield symbolic sequences $S = (s_1, \dots, s_N)$ of length up to $N = 5 \times 10^5$. Before the spin orientation is recorded, a sufficient number of sweeps are performed to ensure that the system is equilibrated. In this regard, for a square lattice with side length $L = 128$, and starting with all spins “up,” and by analyzing the magnetization of the system, we observed an equilibration time of approximately $\tau_{\text{eq}} = 3000$ MC sweeps for the lowest temperature. However, for each system considered, we discarded the first 10^5 sweeps to avoid initial transients.

The aim of this work is to use computer science methods, related to the field of lossless data compression, and apply them to a pivotal model system from statistical mechanics, namely the 2D Ising FM and the continuous FM-to-paramagnet transition found therein. In particular, we want to clarify whether the phase transition can be detected, located, and analyzed numerically with high precision just by looking at entropy and complexity measures derived via data-compression utilities. Being well aware that such AE estimates based on sequence-parsing schemes and data-compression utilities might only be used to obtain upper bounds on the actual entropies of the underlying (finite) symbolic sequences [16,28,31], we compare our findings to those obtained using the BE estimators that here serve as a benchmark.

The remainder of this article is organized as follows. In Sec. II we introduce the information-theoretic observables obtained from the limiting behavior of block entropies and we detail the LZ string-parsing and data-compression based entropy measures. In Sec. III we discuss the results obtained by applying the aforementioned entropy estimators and in Sec. IV we conclude with a summary.

II. INFORMATION-THEORETIC OBSERVABLES FOR SYMBOLIC SEQUENCES

In Sec. II A we introduce the basic notation from information theory, subsequently used to define the entropy rate, excess entropy, and further related measures that might be associated to a 1D symbolic sequence of finite length. Regarding the definition of the entropy rate and excess entropy, we follow the notation used in Refs. [4,5,21], where a more elaborate

discussion of the individual information-theoretic observables can be found. In Sec. II B we further introduce the LZ string-parsing scheme and data-compression based entropy measures considered in the remainder.

A. Block entropy, entropy rate, and complexity

Given a symbolic sequence S of finite length N , i.e., $S = (s_1, s_2, \dots, s_N)$, where the individual symbols s_i assume a symbolic value randomly drawn from an alphabet \mathcal{A} of finite size. Here, an individual symbol signifies the outcome of a measurement on a random variable, i.e., the orientation of a single Ising spin at a given point in (simulation) time. Therefore, unless otherwise specified, \mathcal{A} will denote the binary alphabet $\{-1, +1\}$. For s^M denoting a particular symbol block of length $M > 0$, the M -block Shannon entropy, also called BE, a prerequisite needed to define the subsequent information-theoretic observables, reads

$$H_{\text{BE},M}[S] \equiv - \sum_{s^M \in \mathcal{A}^M} \text{Pr}(s^M) \log_2[\text{Pr}(s^M)], \quad (1)$$

wherein $\text{Pr}(s^M)$ specifies the joint probability for blocks of M consecutive symbols. Hence, considering a finite sequence, $\text{Pr}(s^M)$ represents the empirical rate of occurrence of s^M in the given sequence. Consequently, $H_{\text{BE},M}$ depends on the spin-flip dynamics of the chosen Ising spin, implemented by the simulation procedure for the 2D Ising FM, over intervals of M consecutive time steps. In the above formula, the sum runs over all possible M blocks, i.e., combinations of M consecutive symbols, that might be composed by means of the alphabet \mathcal{A} (considering a binary alphabet, there are 2^M such blocks) and we imply to set $0 \log_2(0) \equiv 0$. In general, $H_{\text{BE},M}$ is a nondecreasing function of M , bounded by $H_{\text{BE},M} \leq M \log_2 |\mathcal{A}|$. The upper bound is attained in the limit of sequence length $N \rightarrow \infty$ if the probability of a string factorizes and each letter has the same probability of occurrence, i.e., $\text{Pr}(s^M) = 1/|\mathcal{A}|^M$. In the limit of large block sizes and sequence lengths N , $H_{\text{BE},M}$ might thus not converge to a finite value. As a remedy, due to the above bounding value, the *entropy rate*

$$h \equiv \lim_{M, N \rightarrow \infty} H_{\text{BE},M}[S]/M \quad (2)$$

might be considered instead. It specifies the asymptotic rate of increase of the M -block Shannon entropy with block length M , and, in the limit of large block size and sequence length, indicates an upper bound on the number of bits needed to encode a symbol of the observed sequence. At this point bear in mind that we aim to analyze binary time series, i.e., 1D symbolic sequences that represent the orientation of a single spin located on an instance of a 2D square lattice Ising FM with side length $L = 128$. In this regard, note that Eq. (2), i.e., the M -block Shannon entropy for 1D symbolic sequences, does not converge to the *true* entropy density of the *full* 2D Ising FM. However, this is not an issue since our goal is to locate the critical point T_c , not to provide an accurate entropy measure for the full 2D Ising FM.

In most practical applications the finite length of the underlying symbolic sequences imposes certain sampling issues related to subsequences of a long enough length M ,

rendering it unfeasible to proceed towards very large block sizes. For example, for sequences of length N , where symbols are independent and identically distributed (iid), one might experience a severe undersampling of M blocks if, at a given alphabet size $|\mathcal{A}|$, M is too large or N is too short. In particular, a naive upper bound M_{\max} might be obtained from the constraint $N \geq M2^M$ [28,31]. Consequently, it is desirable to consider proper finite- M approximations to the entropy rate observed for sequences of finite length N , referred to as *apparent entropy rates*. Two such estimators are given by the *per symbol M-BE*

$$h'_{\text{BE},M}[S] = H_{\text{BE},M}[S]/M \quad (3)$$

and the discrete derivative of Eq. (2), defining the entropy rate as a BE increment via

$$h_{\text{BE},M}[S] = H_{\text{BE},M}[S] - H_{\text{BE},M-1}[S] \quad (4)$$

for sequences of finite length N and both equations presuming $M \geq 1$. Viewed as a function of block size, the finite M estimates of the entropy rates converge to the asymptotic value h from above. Hence, considering small block sizes, the underlying symbolic sequences tend to look more random than in the limit $M \rightarrow \infty$. Finally, note that the entropy rate is a measure of *randomness* that might be attributed to the underlying sequences [3,5]. Here, for sequences of finite size N and for a maximally feasible block size M_{\max} we denote the BE based estimate of the entropy rate as

$$h_{\text{BE}}[S] \equiv h_{\text{BE},M_{\max}}[S]. \quad (5)$$

For 1D symbolic sequences, there are three different but equivalent expressions to define the excess entropy. These are based on the convergence properties of the entropy rate, the subextensive part of the BE in the limit of large block sizes and the mutual information between two semi-infinite blocks of variables; see Refs. [4,9]. Here we focus on the definition of the excess entropy, also termed “effective measure complexity” [2,21,32], related to the convergence properties of the entropy rate in the form

$$C_{\text{BE}}[S] = \sum_{M=1}^{\infty} (h_{\text{BE},M}[S] - h_{\text{BE}}[S]). \quad (6)$$

As pointed out above, the conditional entropies $h_{\text{BE},M}[S]$ constitute upper bounds on the asymptotic entropy rate, allowing, in principle, for an improving estimate of h_{BE} for increasing M . Note that since the sum in Eq. (6) extends to $M \rightarrow \infty$, it implies the limit $N \rightarrow \infty$ and $h_{\text{BE}}[S] = h$. However, for practical purposes, i.e., since we consider sequences of finite length N only, the sum in Eq. (6) needs to be truncated at a maximally feasible block size M_{\max} that still yields a reliable estimate of h (see discussion above). Hence, for a symbolic sequence S of finite length N , $C_{\text{BE}}[S]$ accounts for the randomness that is present at small values of M that vanishes in the limit of large block sizes. The excess entropy is considered a measure of *statistical complexity* [3,5] with the ability to detect structure within the considered sequences [2]. It satisfies the desirable “one-hump” criterion, according to which a proper measure for statistical complexity yields a small numerical value for highly ordered and highly disordered sequences [33–37], thereby keeping the ability

to distinguish configurations that exhibit similar randomness but are structurally distinct [3]. Further, note that also other practically computable approaches exist, which indeed seem to measure complexity as expected [2,32,38].

For 1D symbolic sequences, a further information-theoretic observable, termed *multi-information* [39] is given by the first summand in Eq. (6), i.e.,

$$I_{\text{BE}}[S] = h_{\text{BE},1}[S] - h_{\text{BE}}[S]. \quad (7)$$

Albeit I_{BE} is closely related to the excess entropy C_{BE} (this holds only in the limit of large block sizes M ; see Ref. [39] for a more general discussion of the multi-information), it captures a particular contribution to the convergence of the entropy density. In this regard, for sequences of infinite length, i.e., in the limit $N \rightarrow \infty$, it measures the decrease of the entropy rate observed by switching from the level of single variables (1-block) statistics to the statistics attained as $M \rightarrow \infty$. Recently, the multi-information was introduced and used to characterize spin configurations for the 2D Ising FM in the thermodynamic limit by analytic means [39]. It was found to exhibit an isolated global maximum right at the critical temperature T_c and thus also satisfies the “one-hump” criterion desired for the full complexity measure. For completeness, note that an early study, focused on computing an information-theoretic complexity measure for the 2D Ising FM was presented by Ref. [40]. Also, quite recently, Ref. [41] reported on different ways to decompose the entropy of a 2D lattice system into sums of conditional entropies. Also note that a complementary approach, focused on carefully carving out information-theoretic aspects of the 2D Ising model in terms of mutual information, was presented by Ref. [42].

B. String-parsing and data-compression based entropy measures

Below we illustrate the LZ string-parsing scheme and the data-compression tools used to implement entropy measures by algorithmic means.

Lempel-Ziv string-parsing scheme. The LZ string-parsing scheme considered here is based on a coarse graining of the input sequence S , yielding a quantity termed “LZ” complexity. Therefore, the input sequence is split into several independent blocks. By traversing the input sequence, a new block is completed whenever one encounters a new subsequence of consecutive symbols that does not match a subsequence of the already traversed part of the input sequence.

More formally, given the symbolic sequence $S = (s_1, \dots, s_N)$, for which the subsequence (s_i, \dots, s_j) might be specified as $S(i, j)$, we obtain a parsed sequence S' using the following procedure.

(1) Initialize the parsed sequence $S' = (s_1)$ and an empty auxiliary sequence $Q = ()$. Traverse the sequence S from left to right, using an index i initialized as $i = 1$.

(2.1) In step i , advance i to $i + 1$ and extend the auxiliary sequence Q via symbol s_{i+1} .

For example, after increasing $i = 1 \rightarrow i = 2$, one has $Q = (s_2)$. More general, if the auxiliary sequence already reads $Q = (s_j, \dots, s_i)$, it is extended to $Q = (s_j, \dots, s_i, s_{i+1})$.

(2.2) Check whether the current auxiliary sequence Q matches any subsequence of $S(1, i)$. If not, append the auxiliary

sequence Q as a new “block” to the parsed sequence S' and reset $Q = ()$.

For example, in step (1) one has $Q = (s_2)$. If Q does not match the symbol $S(1,1) = s_1$, then set $S' = (s_1)(s_2)$ and reset $Q = ()$.

(3) Repeat (2.1) and (2.2) until $i = N$ and append Q to S' to yield the final parsing S' .

Finally, the LZ complexity $N_{\text{LZ}}[S]$ associated with sequence S is simply the number of consecutive blocks found after the coarse-graining procedure is completed [29]. As an example, consider the sequence $S = 1010000110$. Following the above procedure yields the parsed sequences $S' = (1)(0)(100)(001)(10)$ for which the LZ complexity reads $N_{\text{LZ}}[S] = 5$.

The LZ complexity provides means to quantify the degree of order or disorder in an observed symbolic sequences [28,29]. Therefore, the term complexity is somewhat misleading in our context. As pointed out in Ref. [28], a proper normalization makes it possible to relate the LZ complexity to the entropy rate of the symbolic sequence, i.e.,

$$h_{\text{LZ}}[S] = \lim_{N \rightarrow \infty} h_{\text{LZ}}[S] = \lim_{N \rightarrow \infty} \frac{N_{\text{LZ}}[S] \ln(N)}{N}. \quad (8)$$

Note that in Ref. [28] two different variants of LZ parsing are considered; here we use the parsing scheme that that reference refers to as LZ 77.

The above string-parsing scheme might also be used to compute an observable that closely follows the definition of the BE based excess entropy. Therefore, bear in mind that in the definition of the excess entropy Eq. (6), the individual terms involve the entropy-rate estimates $h_{\text{BE},M}$ for finite block size M , i.e., containing symbol correlations up to length M only. By using the LZ string-parsing scheme, similar estimates of the entropy rate, restricted to feature correlations up to some specified length M , might be obtained by preprocessing the initial sequence by applying a M -block standard random shuffle procedure. Thereby, the initial length- N sequence S is first split into $\lfloor N/M \rfloor$ blocks of length n and possibly a remaining block of length $N \bmod(M)$. Then, these blocks are brought into random order and merged to form the new, M -block shuffled surrogate sequence $S^{(M)} = \text{shuffle}(S, M)$. This maintains the individual symbol frequencies, destroys all correlations that extend over lengths larger than M , and yields a particular realization of a M -block shuffled surrogate sequence. Note, however, that the distribution of M blocks, obtained by sliding a window of length M over the initial sequence and keeping track of all overlapping subsequences of length M (e.g., used to compute M -block entropies), is not conserved by this procedure. The case $M = 1$ corresponds to the standard random shuffling procedure considered in Ref. [43]. Finally, a standard random shuffle based excess entropy (or similar: standard random shuffle based complexity) that utilizes the LZ string-parsing scheme might be obtained as

$$C_s[S] = \sum_{M=1}^{M_{\text{max}}} (h_{\text{LZ}}[S^{(M)}] - h_{\text{LZ}}[S]), \quad (9)$$

where M_{max} indicates a maximal feasible block size for the shuffling procedure. Albeit the above observable is no direct

analog of the excess entropy Eq. (6), it is expected to behave in a similar manner.

Similarly, the string-parsing scheme might be used to compute a shuffling based equivalent of the multi-information [39] Eq. (7) as

$$I_s[S] = h_{\text{LZ}}[S^{(1)}] - h_{\text{LZ}}[S]. \quad (10)$$

Therein, $S^{(1)}$ simply represents a surrogate sequence obtained by a 1-block standard random shuffle [43] which maintains the symbol frequencies but destroys correlations on all scales. Hence, Eq. (10) reflects the entropy overestimate observed by going from a representation of the sequence with no correlations at all to its original representation including all correlations.

Data-compression tools. In addition we also consider three commonly used black-box data compression tools, namely zlib [18], bz2 [19], and lzma [20], in order to compute an AE that is based on the compressibility of the underlying sequence according to

$$h_{\text{alg}}[S] = \frac{\text{length}[\text{compress}(S)]}{N}; \quad (11)$$

see Ref. [16]. According to the latter reference, this data-compression tool based entropy should provide an upper bound on the entropy of the underlying sequences. Note that the shuffling based (approximate) excess entropy and multi-information can also readily be computed using Eq. (11).

III. RESULTS

Subsequently we address two distinct issues: First, in Sec. III A, we assess how well the aforementioned, string-parsing and data-compression based entropy estimators might be used to characterize the FM-to-paramagnet transition in the 2D Ising FM. Therefore, we consider the information-theoretic observables introduced previously in Sec. II and capitalize on their scaling behavior as a function of the system temperature. Since these estimates are obtained by algorithmic means, we here refer to them as “AE estimates.” Second, in Sec. III B, we evaluate how well the AE estimates compare to the more conventional BE estimates and discuss further means to improve on the difference between the respective estimates.

A. Using algorithmic entropy estimates to locate the critical point

In this section we summarize the results on the issue of how well the phase transition in the 2D Ising FM can be resolved by means of the LZ string-parsing scheme [28,29,31], as well as the zlib [18], bz2 [19], and lzma [20] black-box data compression utilities. Therein, we are not interested in the absolute values of the entropy estimates thus obtained, but merely in the data-curve characteristics as function of the system temperature. The final estimates for the transition points, resulting from the considered observables, and their comparison to the literature value of the critical temperature, i.e., $T_c^{\text{lit}} = 2.269$, can be used to assess the value of the AE estimators as easy-to-compute utilities that might yield

valuable information on the structural change as visible in measurements of finite-length symbolic sequences.

1. Lempel-Ziv string-parsing scheme

a. Entropy rate. As pointed out previously, for a given input sequence S , consisting of N consecutive symbols, the LZ string-parsing scheme yields a parsed sequence of length $N_{LZ}[S]$, making it possible to compute the respective entropy rates for sequences of finite length via $h_{LZ,N}[S]$; see Eq. (8). We applied this estimation procedure to ensembles of length- N sequences, accounting for the orientation of a selected spin in a 2D Ising FM at different values of the temperature parameter T , considering various values of N up to $N = 2^{16} = 65\,536$; see Fig. 1(a). Therein, the upper inset of Fig. 1(a) illustrates the change of the average asymptotic entropy rate at $T = 2.267 \approx T_c$ with increasing sequence length N . For the extrapolation to the asymptotic limit, an empirically motivated fit function of the form

$$h_{LZ,N} = h_\infty + [a \log_2(N)]/N^\gamma, \quad (12)$$

motivated in Ref. [31] and also used in Ref. [28], was employed. The main plot of Fig. 1(a) shows the extrapolated asymptotic entropy rates $h_\infty(T)$. The asymptotic entropy rates are in accord with intuition: At low T , the symbolic sequences exhibit a high degree of order; hence, the associated entropy rate is small (vanishing in the limit of perfect order). In contrast, at high T , the sequences exhibit maximal randomness, i.e., subsequent spin orientations in the underlying model are uncorrelated, and the entropy rate tends towards $h_\infty = 1$. Of pivotal interest is the region close to T_c where nontrivial, long-range correlations between the successive orientations of the monitored spin build up. Below it will be of interest to check whether the previously introduced measures of statistical complexity are sensitive to these structural changes and can be used to locate the critical point by means of a finite-size scaling analysis using sequences of different length N . The bottom inset of the figure indicates the change of the fit-parameter γ as function of the temperature. As evident from the figure, in the high-temperature regime above the critical point $T_c = 2.269 \dots$, it assumes a stationary value $\gamma(T > T_c) \approx 0.73(2)$. In the low-temperature regime it exhibits an increasing value with decreasing temperature. Overall, the agreement between the asymptotic entropy rate h_∞ , the entropy rate $h_{LZ,N}$ at $N = 2^{16} = 65\,536$, and the common BE at $h_{BE,N}$ at $N = 10^5$ is remarkably good; see Table I. In particular, for all values of T considered, $h_{LZ,N}$ seems to be a satisfactory approximation to h_∞ , since both values agree within error bars.

b. Excess entropy. Figure 1(b) illustrates the block-shuffling based excess entropy Eq. (9) as function of the system temperature, averaged over a large number of input sequences. In the analysis, we restricted the sum to $M_{\max} = 23$. As evident from the figure, $C_s(T)$ assumes small values for both, the low- T and high- T regimes. In between, i.e., in the paramagnetic phase close to the critical point T_c , it assumes a peak value thus satisfying the naive ‘‘one-hump’’ criterion [3,33]. For an increasing sequence length the peak gets more pronounced and shifts towards T_c . In order to assess whether the position

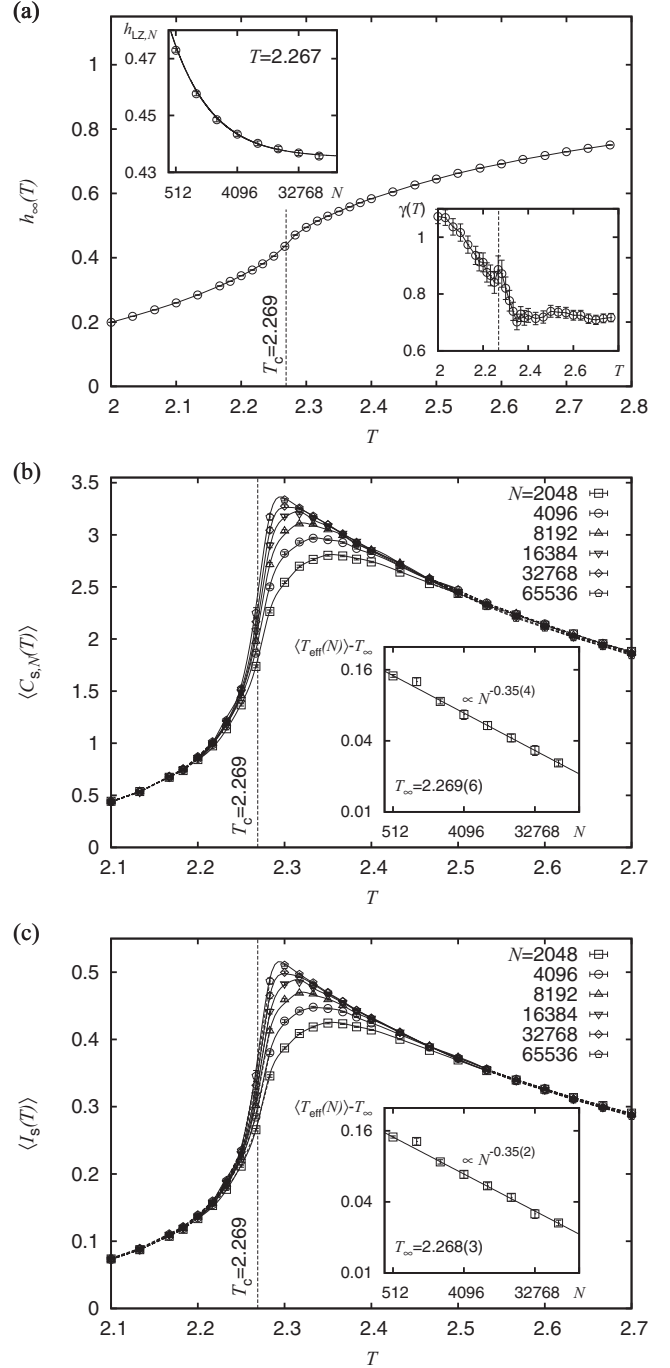


FIG. 1. Results for the information-theoretic observables computed using the LZ sequence-parsing scheme averaged over many input sequences. (a) Extrapolated estimates $h_\infty(T)$ of the entropy rate as function of the system temperature T . The upper inset illustrates the extrapolation of the finite-length entropy-rate estimates $h_{LZ,N}$ at $T = 2.267 \approx T_c$ using the fit function discussed in the text. The lower inset shows the fit exponents $\gamma(T)$ as function of the temperature. (b) Analysis of the block-shuffling based excess entropy, also termed ‘‘complexity,’’ $C_s(T)$. The inset illustrates the extrapolation of the system-size dependent peak locations $T_{\text{eff}}(N)$ to the asymptotic limit. The solid lines indicate cubic spline, fitted to the interval $T \in [2.24, 2.5]$ and the dashed lines are a guide for the eyes only. (c) Analysis of the block-shuffling based multi-information $I_s(T)$ similar to (b).

TABLE I. Comparison of entropy rates for different estimation procedures at different temperatures. From left to right: system temperature T , LZ-parsing based entropy rate $h_{LZ,N}$ at $N = 2^{16} = 65\,536$, LZ-parsing based asymptotic entropy rate h_∞ [extrapolated using Eq. (12)], and BE based estimate $h_{BE,N}$ at $N = 10^5$ (block size 7).

T	$h_{LZ,N}$	h_∞	$h_{BE,N}$
2.2	0.3442(6)	0.3441(5)	0.339(3)
2.267	0.436(1)	0.435(1)	0.428(3)
2.5	0.647(1)	0.645(1)	0.643(2)

of the peak in the asymptotic limit coincides with the critical point, we performed a finite-size scaling analysis.

To accomplish this, we fitted cubic splines to the peak region $T \in [2.24, 2.5]$ of the excess entropy data curves to obtain the respective sequence length dependent, thus “effective,” peak positions $T_{\text{eff}}(N)$. In Fig. 1(b), the fit curves are shown as solid lines (dashed lines are a guide for the eye only). Error bars for the peak position are computed using bootstrap resampling of the underlying data [44]. The asymptotic peak position is then extrapolated using a fit to

$$T_{\text{eff}}(N) = T_\infty + aN^{-b}, \quad (13)$$

yielding $T_\infty = 2.269(6)$, $a = O(1)$, and $b = 0.35(4)$ [reduced $\chi^2(\chi_{\text{red}}^2) = 0.58$], see inset of Fig. 1(b), in good agreement with the literature value $T_c \approx 2.269$. Albeit not shown here, we further observe that the fluctuations $N\text{var}(C_s)$ are peaked directly at T_c .

At this point, bear in mind that we study symbolic sequences that represent the time series of the orientation of a selected spin, recorded for N MC sweeps on a 2D square lattice of finite side length $L = 128$. Analyzing the specific heat $C = (k_B T^2)^{-1}[\langle E^2 \rangle - \langle E \rangle^2]$ [30] of the $L = 128$ 2D Ising FM we find an accentuated peak at $T_{\text{peak}} = 2.278(1)$, indicating the “effective” location of the critical point for the finite system (not shown). Note that this value is slightly larger than the asymptotic critical point $T_c = 2.269 \dots$. Here we obtain the interesting result that, by performing a scaling analysis for the excess entropy peak locations for symbolic sequences of different length N (all for the finite system size $L = 128$), the results seem to extrapolate towards T_∞ , which is in striking agreement with the asymptotic critical point T_c . However, the results are also in reasonable agreement with the effective critical point suggested by the specific heat. Hence, within the precision reached by our current analysis we cannot completely rule out that the results extrapolate towards T_{peak} instead of the asymptotic critical point T_c .

c. Multi-information. The results for the standard random shuffle based multi-information Eq. (10) are shown in Fig. 1(c).

Here a finite-size scaling analysis of the effective peak positions, again obtained by fitting cubic splines to the peak region $T \in [2.24, 2.5]$ of the data curves, using bootstrap resampling to compute error bars and Eq. (13) to extrapolate to the asymptotic limit, yields the estimates $T_\infty = 2.268(5)$, $a = O(1)$, and $b = 0.34(2)$ ($\chi_{\text{red}}^2 = 0.16$). Similar to the findings for the excess entropy, the estimate of T_∞ is in good agreement with the known value of T_c , indicating that I_s is highly sensitive to the correlations that emerge close to the critical

point. However, note that albeit the multi-information is able to resolve the FM-to-paramagnet transition in the 2D Ising FM considered here, it is by no means a universal measure to reliably detect any order-disorder transition. Since it is based on 1D symbolic sequences that relate to a single spin, it neglects nontrivial correlations between adjacent spins on the lattice. Consequently, as presented here, it is not able to distinguish pure ferromagnetic order from, say, perfect antiferromagnetic order.

d. S measure. For the purpose of comparing an observable M computed for symbolic sequences of finite length to their surrogate counterparts, Ref. [43] employed the \mathcal{S} measure

$$\mathcal{S}[S] = \frac{|M_{\text{orig}}[S] - \langle M_{\text{surr}}[S] \rangle|}{\text{sDev}(M_{\text{surr}}[S])}. \quad (14)$$

Therein, in order to quantify a significant deviation between both observables, it states the difference between the observable for the original sequence to the average value of the observable for an ensemble of proper surrogates, measured in units of the standard deviation found for the surrogate ensemble. Here, to probe the sensitivity of the \mathcal{S} measure to structural changes in the symbolic sequences at different temperatures, we choose as an observable the LZ complexity based estimator for the entropy rate. That is, for a given sequence S we consider $M_{\text{orig}}[S] = h_{LZ}[S]$ and $M_{\text{surr}}[S] = h_{LZ}[S^{(1)}]$ (note that this corresponds to the construction procedure 1 for surrogate sequences in Ref. [43]), using 10^2 surrogate sequences for averaging obtained by standard random shuffling. In Eq. (14), the average $\langle \cdot \rangle$ and standard deviation $\text{sDev}(\cdot)$ are computed from 100 independent surrogate sequences. Figure 2 illustrates the \mathcal{S} measure, averaged over different (original) sequences for various values of N . As evident from the figure, the \mathcal{S} measure exhibits an isolated peak close to the critical point. This does not come as a surprise: Albeit normalized by a temperature dependent quantity, the numerator effectively

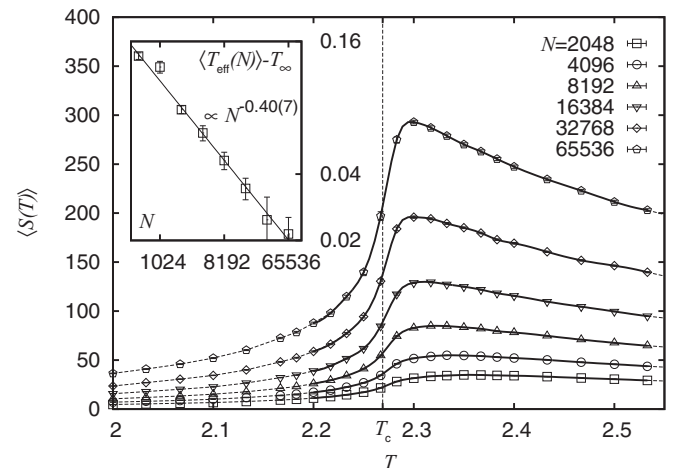


FIG. 2. Results for the \mathcal{S} measure as discussed in the text, averaged over many input sequences. The main plot illustrates the \mathcal{S} measure for the LZ-parsing based entropy rate, considering a standard random shuffle to obtain the surrogate sequences used to compute Eq. (14). The solid lines represent cubic splines, fitted to the interval $T \in [2.2, 2.55]$ and the dashed lines are a guide for eyes, only. The inset shows the finite-size scaling analysis performed to extrapolate the asymptotic peak location T_∞ .

matches the random shuffle based multi-information Eq. (10). Here a finite-size scaling analysis of the system-size dependent peak locations (obtained by fitting cubic splines to the data points in the interval $T \in [2.2, 2.55]$) yields $T_\infty = 2.277(10)$, $a = O(1)$, and $b = 0.40(7)$ ($\chi_{\text{red}}^2 = 1.11$), in agreement with the above results.

2. Common data-compression utilities

In the previous section we analyzed three different observables that appear to be very sensitive to structural changes in the symbolic sequences of finite length as the critical point of the underlying model is approached. These were the standard random shuffle based excess entropy (also termed complexity), multi-information, and the S measure for the LZ-parsing based entropy rate. Subsequently, we restrict our further analysis to the shuffling based multi-information since it is very simple to compute and seems to be able to detect and quantify structural changes in the recorded sequences that might be used to locate the phase transition point of the underlying model with ease. Furthermore, it has a clear-cut interpretation: It yields the entropy rate difference observed for a symbolic sequence including all symbol correlations and a surrogate sequence featuring the same symbol frequencies without correlations.

As pointed out above, we here consider three commonly used black-box data compression tools, namely zlib [18], bz2 [19], and lzma [20], in order to compute an AE that is based on the compressibility of the underlying sequence according to Eq. (11); see Ref. [16].

a. Results obtained using zlib. The results obtained by implementing the `compress()` statement in Eq. (11) by using the zlib data-compression tool [18] is shown in Fig. 3(a). Therein, by fitting the peaks using cubic splines and extrapolating to the asymptotic limit via Eq. (13) we yield $T_\infty = 2.278(5)$, $a = O(1)$, and $b = 0.5(1)$ (reduced chi-square $\chi_{\text{red}}^2 = 1.31$), slightly overestimating the literature value of the critical point T_c but still within a distance of 2σ . For comparison, the results obtained by fitting polynomials of order 8 to the data curves are listed in Table II. Regarding the characteristics of the data curves, note that albeit the peak location monotonously decreases towards a value in decent agreement with T_c , the peak height seems to first increase to a value $\langle I_s(T_{\text{eff}}) \rangle \approx 0.55$ for $5000 \leq N \leq 15000$. For larger value of N , the peak height seems to decrease again.

b. Results obtained using bz2. Implementing the `compress()` statement in Eq. (11) by using the bz2 data-compression tool [19] is shown in Fig. 3(b). Therein, by fitting the peaks using cubic splines and extrapolating to the asymptotic limit, we yield $T_\infty = 2.26(1)$, $a = O(1)$, and $b = 0.28(7)$ ($\chi_{\text{red}}^2 = 0.40$), in agreement with the literature value of the critical point T_c . Again, for comparison, the results obtained by fitting polynomials of order 8 to the data curves are listed in Table II. As evident from Fig. 3(b), and in contrast to the results obtained using the zlib tools, the peak of data curves behaves similar to the multi-information considered in the context of the LZ-parsing scheme. That is, the peak consistently shifts towards T_c and the peak height also increases with increasing N (however, we made no attempt to quantify the latter).

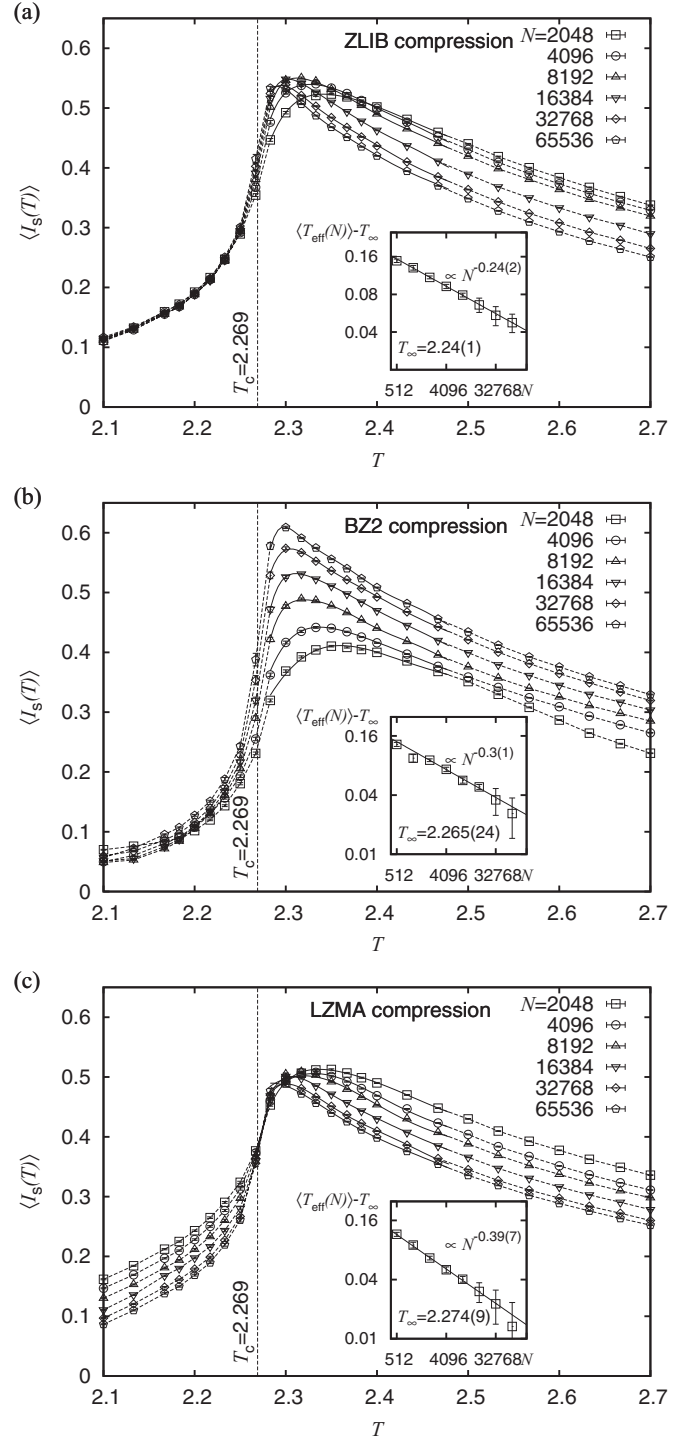


FIG. 3. Results for the standard random shuffle based multi-information computed using three black-box data-compression utilities, averaged over many input sequences. The subfigures illustrate the analysis of the shuffling based multi-information using the AE, where the `compress()` part is implemented using (a) the zlib data-compression tool, (b) the bz2 data-compression tool, and (c) the lzma data-compression tool. In the main figures, the solid lines indicate fits to polynomials of order 8, fitted to the interval $T \in [2.24, 2.45]$ and the dashed lines are a guide for eyes, only. The insets show the extrapolation of the system size dependent peak locations to the asymptotic limit using Eq. (13).

TABLE II. List of the asymptotic critical points T_c and scaling exponents b , estimated from the finite-size scaling [see Eq. (13)] of the peak locations associated to the standard random shuffle based multi-information, implemented by means of the zlib, bz2, and lzma data-compression utilities. Therein, the peaks were fit by cubic splines (CS) and polynomials of order 8 (P8). To facilitate comparison, note that the known critical temperature of the 2D Ising FM reads $T_c = 2.269\dots$

	CS		P8	
	T_∞	b	T_∞	b
ZLIB	2.278(5)	0.5(1)	2.24(1)	0.24(2)
BZ2	2.26(1)	0.28(7)	2.265(4)	0.31(12)
LZMA	2.276(4)	0.41(5)	2.274(9)	0.39(7)

c. Results obtained using lzma. Last, implementing the compress(·) statement in Eq. (11) by using the lzma data-compression tool [20] is shown in Fig. 3(c). Therein, by fitting the peaks using splines and extrapolating to the limit $N \rightarrow \infty$ yields $T_\infty = 2.276(4)$, $a = O(1)$, and $b = 0.41(5)$ ($\chi_{\text{red}}^2 = 0.29$), in decent agreement with the literature value of the critical point T_c . As can be seen from Table II, the results obtained using a fitting procedure by means of polynomials of order 8 compare even better to T_c . Note that here, the peak gets narrower with increasing sequence length N with the peak location shifting towards a value consistent with T_c . However, here the effect already observed for the zlib tool, i.e., a decreasing peak height for increasing N , is even more pronounced.

B. Comparison of algorithmic entropy estimates to block entropies

A further issue we addressed is the question of how well the different entropy estimates (based on the LZ string-parsing scheme and the three data-compression utilities discussed earlier), compare to more conventional BE estimates, obtained using well-established procedures; see Sec. II and Refs. [5,9].

Here, in order to prepare reference values for the entropy rate Eq. (4) using the BE estimator Eq. (1) we considered sequences of length $N = 10^5$ and a maximally feasible block size $M_{\text{max}} = 7$, i.e., $h_{\text{BE}} \equiv h_{\text{BE}}[7] = H_{\text{BE}}[7] - H_{\text{BE}}[6]$. As noted earlier, for iid sequences one might experience a severe undersampling of M blocks if, at a given alphabet size, M is too large or N is too short. In particular, a naive upper bound M_{max} might be obtained from the constraint $N \geq M2^M$ [28,31]. Here, using $M_{\text{max}} = 7$ and $N = 10^5$ we checked that $h_{\text{BE}}[7]$ has converged properly for all considered temperatures. Albeit this provides only an upper bound on the true entropy rate, it might nevertheless yield a reasonable approximation to the actual entropy of the considered sequences.

1. Lempel-Ziv string-parsing scheme

At first we compared the LZ string-parsing based entropy rate estimates to those obtained using the BE estimator. Thereby we performed a comparison to the entropy rates observed for sequences of finite length $N = 65\,536$ and to the asymptotic estimates h_∞ , resulting from extrapolation via

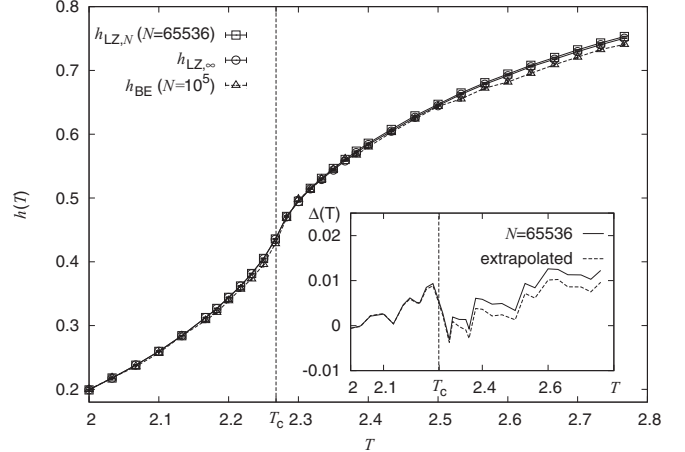


FIG. 4. Comparison of the LZ string-parsing scheme based entropy rates to those obtained using a well-established BE measure. The main plot contrasts the data curves of $h_{\text{LZ},N}(T)$ (at $N = 65\,536$), the asymptotic estimate $h_{\text{LZ},\infty}(T)$, and the BE based estimate $h_{\text{BE},N}(T)$ (at $N = 10^5$) as function of the system temperature T . The inset gives an account of the difference $\Delta(T)$, referred to in the text.

Eq. (12). The results are illustrated in Fig. 4. Therein, the main plot shows the entropy rates $h_{\text{LZ}}(T)$ and $h_{\text{BE}}(T)$ as functions of the system temperature T for the different estimators. The inset indicates the difference,

$$\Delta(T) = h_{\text{LZ}}(T) - h_{\text{BE}}(T), \quad (15)$$

between the respective string-parsing based entropy rate to the BE estimates. As evident from the figure, the absolute difference is typically smaller than 0.01 with the largest deviation close to the critical point T_c . While both estimates compare similarly well to the BE estimate at low temperatures $T < T_c$, the extrapolated result h_∞ is slightly closer to h_{BE} for $T > T_c$.

2. Common data-compression utilities

As reported in the previous paragraph and illustrated in Fig. 4, the LZ string-parsing based entropy rate compares astonishingly well to those estimates obtained using the BE estimator (even for sequences of finite length $N = 65\,536$). Now, by considering the AE rate estimator Eq. (11), implemented using the three data-compression utilities discussed earlier, we find that the entropy-rate estimates for binary sequences of length $N = 10^5$ significantly overestimate the results obtained via the BE estimator; see the data curves for $m = 1$, i.e., $|\mathcal{A}| = 2$ (see discussion below), in Figs. 5(a)–5(c). As mentioned earlier and pointed out in Ref. [16], the AE rate Eq. (11) provides only an upper bound on the true entropy rate of the underlying process. In order to explore possible routes that might support a more reliable entropy estimate, we next study auxiliary sequences of length N , consisting of iid symbols, taken from a more general alphabet of size $|\mathcal{A}|$ instead of binary sequences only.

In Fig. 6, we compare the entropy rates obtained via Eq. (11) using the three data-compression tools—zlib, bz2, and lzma—to the value $\log_2(|\mathcal{A}|)$ expected for such iid

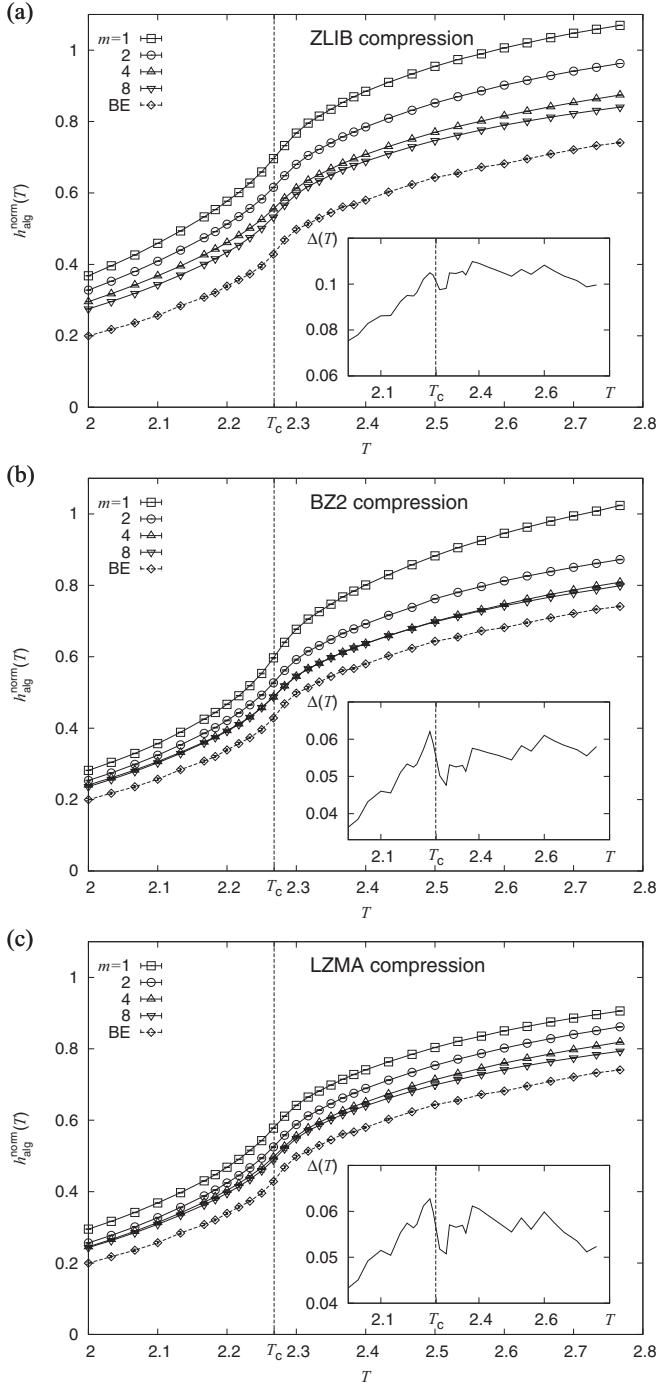


FIG. 5. Comparison of the data-compression based entropy-rate measures to those obtained using a well-established BE measure. The main plot contrasts the data curves of the normalized entropy estimate $h_{\text{alg}}^{\text{norm}}(T)$ (at $N = 10^5$), to the block-entropy based estimate $h_{\text{BE}}(T)$ as function of the system temperature T and different neighborhood-template sizes M , as discussed in the text. The inset gives an account of the difference $\Delta(T)$, referred to in the text.

sequences. As evident from the figure, the respective ratio approaches unity for increasing alphabet size and for N not too small. For example, for $|\mathcal{A}| = 2$ and for large $N > 10^5$, the respective estimates read $h_{\text{alg}}/\log_2(2) \approx 1.27$ (zlib), $h_{\text{alg}}/\log_2(2) \approx 1.24$ (bz2), $h_{\text{alg}}/\log_2(2) \approx 1.07$ (lzma). For

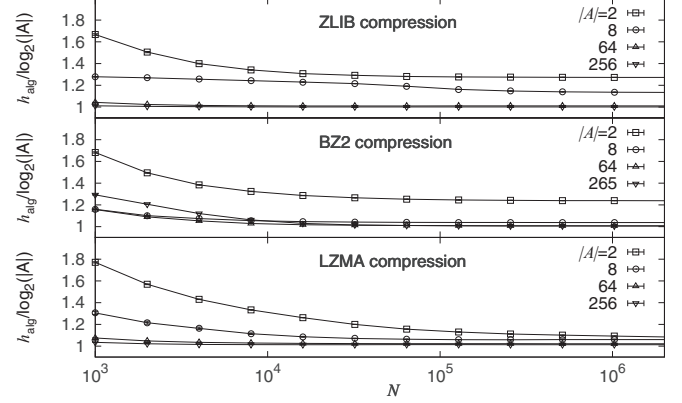


FIG. 6. Comparison of the compression-based entropy-rate estimates for iid sequences considering the three different data-compression tools and alphabet sizes $|\mathcal{A}| = 2, 8, 64, 256$. For increasing alphabet size, the estimate of the entropy rate for a given sequence length approach the estimate $\log_2(|\mathcal{A}|)$.

the larger alphabet size $|\mathcal{A}| = 256$ the respective estimates read $h_{\text{alg}}/\log_2(256) \approx 1.0003$ (zlib), $h_{\text{alg}}/\log_2(256) \approx 1.004$ (bz2), $h_{\text{alg}}/\log_2(256) \approx 1.07$ (lzma). Albeit these results are valid only for iid sequences, we might nevertheless expect to find a tighter upper bound on the entropy rate for symbolic sequences with possibly long-range correlations by simply increasing the alphabet size $|\mathcal{A}|$.

This can be achieved in the following manner. Instead of monitoring the orientation of a single spin during the simulation of the 2D Ising FM, we monitor the orientation of a number of, say, m spins, located within a neighbor template of size m , as introduced in Ref. [10] (to analyze the local entropy in a frustrated 2D spin system) and used in Ref. [12] to systematically parse a 2D configuration of spins into 1D sequences of length m . These can then be interpreted as a binary representation of a particular symbol from an alphabet of size $|\mathcal{A}| = 2^m$. Following this approach, we show in Fig. 6 the estimates for the entropy rates obtained by considering neighborhood templates of size $m = 1, 2, 4, 8$, i.e., alphabet sizes $|\mathcal{A}| = 2, 4, 16, 256$, to construct symbolic sequences of length $N = 10^5$. So as to be able to compare these values to those obtained by means of the BE based estimates (monitoring the orientation of a single spin), we normalize the plain AE estimates resulting from Eq. (11) using $\log_2(|\mathcal{A}|)$. That is, we compute

$$h_{\text{alg}}^{\text{norm}}[S] = \frac{h_{\text{alg}}[S]}{\log_2(|\mathcal{A}|)} \equiv \frac{\text{length}[\text{compress}(S)]}{\text{length}[\text{compress}(S_{\text{id}})]}, \quad (16)$$

where S_{id} signifies a iid sequence with the same length and alphabet size as S . The insets illustrate the difference between $h_{\text{alg}}^{\text{norm}}$ and h_{BE} for an alphabet size $|\mathcal{A}| = 256$ as function of the system temperature. As evident from the Figs. 5(a)–5(c), the estimates for increasing alphabet size indeed approach the BE based estimates. Thereby, the difference $\Delta(T)$ seems to be smallest at low temperatures and increases towards higher temperatures, fluctuating around a plateau value for $T > T_c$. Overall, the lzma estimator seems to perform best, exhibiting $\Delta \approx 0.05$ – 0.06 for $T > T_c$, while the zlib based estimator performs worst, exhibiting $\Delta \approx 0.09$ – 0.11 for $T > T_c$. For

comparison, close to the critical point, i.e., at $T = 2.267$, we find $h_{\text{BE}} = 0.461(7)$, $h_{\text{alg}}^{\text{norm}} = 0.532(1)$ (zlib), $h_{\text{alg}}^{\text{norm}} = 0.487(1)$ (bz2), $h_{\text{alg}}^{\text{norm}} = 0.4884(6)$ (lzma).

IV. SUMMARY

In this article we considered information-theoretic observables to analyze short symbolic sequences, comprising binary time series that represent the orientation of a single spin in the 2D Ising FM, for different system temperatures T . The latter were chosen from the interval $T \in [2, 2.8]$, enclosing the critical point $T_c \approx 2.269$ of the model. Here our focus was set on the estimation of the entropy rate via (i) a LZ based string-parsing scheme and (ii) common data-compression utilities (in particular, zlib [18], bz2 [19], and lzma [20]). These approaches require a much smaller computational effort compared to the standard BE approach. Furthermore, they can be considered as simple yet useful versions of “algorithmic” entropy calculations which, in principal, seek the shortest of all programs generating a given sequence. In comparison to a “model-tailored” analysis in terms of methods from statistical mechanics, the presented information-theoretic approach is model independent. Thus, the principal observables and analysis methodology might also be applied to other kinds of order-disorder transitions; see, e.g., [12] for an analysis of ground-states for the 2D random bond Ising model and the 3D random field Ising magnet. Further, a slight generalization of the monitored random variables that yield the symbolic “input” sequences, e.g., via neighbor templates comprising groups of adjacent spins, might be used to also resolve spatial structure that possibly extends over several lattice spacings; see, e.g., [9].

In a first analysis we demonstrated that certain standard random shuffle based variants of the excess entropy, multi-information as well as an entropy-rate related \mathcal{S} measure might be used to obtain reasonable estimates for the critical point of the underlying model. Albeit we obtained good results for all three observables when considering the LZ string-parsing scheme, we restricted our analysis of the common data-compression tools to the multi-information I_s since it was easy to compute by means of black-box data compression utilities. As evident from Table II, the estimated critical temperatures, obtained by an extrapolation of the multi-information peak location via Eq. (13), compare well to the known critical temperature. As pointed out earlier, we here obtain the interesting result that, by performing a scaling analysis for the multi-information peak locations for symbolic sequences of different length N (all for the finite system size $L = 128$), the results seem to extrapolate towards values T_∞ (see Table II), which are in striking agreement with the asymptotic critical point T_c . However, the results are also in reasonable agreement with the effective critical point T_{peak} , indicated by the accentuated peak of the specific heat for the $L = 128$ square lattice. Hence, within the precision reached by our current analysis we cannot completely rule out that the results extrapolate towards T_{peak} instead of the asymptotic critical point T_c . Note that an unrelated study (Ref. [45]), where a data-compression tool for the recognition of magnetic phases

was designed (based on a different algorithmic procedure and using different observables to locate the critical point), found $T_c \approx 2.29$ (for $L = 128$) and $T_c \approx 2.28$ (for $L = 256$) and loosely concludes that the findings extrapolate to the known asymptotic critical point. Also note that conceptually similar analyses, considering BE based observables carried out on 2D configurations of spins obtained from a simulation of the 2D Ising FM, reported in Ref. [4], conclude that the excess entropy is peaked at a temperature $T_c \approx 2.42$ in the paramagnetic phase slightly above the true critical temperature. Similar results on the mutual information [5] for the 2D Ising FM (and more general classical 2D spin models) where recently presented in Ref. [11]. Therein, the authors conclude that the mutual information reaches a maximum in the high-temperature paramagnetic phase close to the system parameter $K = J/k_B T \approx 0.41$ (for $J = k_B = 1$ this corresponds to $T \approx 2.44$). Our new results and analyses, which go beyond the cited literature are presented in our main result part, Sec. III.

In a second analysis we first prepared benchmark data curves for the asymptotic entropy rate of the symbolic sequences via a BE based approach. Subsequently, we compared the results of the various AE estimators to the latter. We found that the LZ string-parsing scheme yields entropy-rate estimates (for finite sequence length and extrapolated to the asymptotic limit) that compare surprisingly well to the benchmark data curves. Further, for the data-compression based estimators we discussed an approach that makes it possible to increase the size of the alphabet \mathcal{A} from which symbols are drawn by monitoring a neighborhood template [10,12], instead of a single spin only. This was motivated by the observation that data-compression based estimators strongly overestimate the entropy rates used as a benchmark. Consequently, symbolic sequences obtained by means of the amended approach encode temporal as well as spatial correlations between the orientation of the spins within the chosen neighborhood template. We found that for an increasing alphabet size, the normalized entropy rates for the sequences approach get closer to the benchmark estimates, supporting the intuition previously gained by analyzing iid sequences. However, the observed difference between both might be due to the finite dictionary size employed during the data-compression procedures and hence the inability of the data-compression based estimators to take advantage of long-range correlations in the symbolic sequence. In principle, we found that the lzma (zlib) based entropy-rate estimator performs best (worst).

ACKNOWLEDGMENTS

O.M. acknowledges financial support from the DFG (Deutsche Forschungsgemeinschaft) under Grant No. HA3169/3-1. The simulations were performed at the HPC Cluster HERO, located at the University of Oldenburg (Germany) and funded by the DFG through its Major Instrumentation Programme (Grant No. INST 184/108-1 FUGG) and the Ministry of Science and Culture (MWK) of the Lower Saxony State.

- [1] N. Goldenfeld, *Lectures On Phase Transitions And The Renormalization Group* (Westview Press, Jackson, TN, 1992).
- [2] P. Grassberger, *Phys. A (Amsterdam, Neth.)* **140**, 319 (1986).
- [3] D. P. Feldman and J. P. Crutchfield, *Phys. Lett. A* **238**, 244 (1998).
- [4] D. P. Feldman, C. S. McTague, and J. P. Crutchfield, *Chaos* **18**, 043106 (2008).
- [5] J. P. Crutchfield and D. P. Feldman, *Chaos* **13**, 25 (2003).
- [6] J. P. Crutchfield and K. Wiesner, *Physics World* **23**, 36 (2010).
- [7] D. V. Arnold, *Complex Syst.* **10**, 143 (1996).
- [8] J. P. Crutchfield and D. P. Feldman, *Phys. Rev. E* **55**, R1239 (1997).
- [9] D. P. Feldman and J. P. Crutchfield, *Phys. Rev. E* **67**, 051104 (2003) (a summary of this article is available at papercore.org; see <http://www.papercore.org/Feldman2003>).
- [10] M. D. Robinson, D. P. Feldman, and S. R. McKay, *Chaos* **21**, 037114 (2011).
- [11] J. Wilms, M. Troyer, and F. Verstraete, *J. Stat. Mech.* (2011) P10011.
- [12] O. Melchert and A. K. Hartmann, *Phys. Rev. E* **87**, 022107 (2013).
- [13] A. N. Kolmogorov, *Indian J. Stat. A* **25**, 369 (1963).
- [14] G. Chaitin, *Algorithmic Information Theory* (Cambridge University Press, New York, 1987).
- [15] J. Machta, *Complexity* **11**, 46 (2006).
- [16] W. Ebeling, *Phys. D (Amsterdam, Neth.)* **109**, 42 (1997).
- [17] A. Puglisi, D. Benedetto, E. Caglioti, V. Loreto, and A. Vulpiani, *Phys. D (Amsterdam, Neth.)* **180**, 92 (2003).
- [18] The *zlib* utilities comprise a general purpose data-compression library. Here we used *zlib* version 1.2.3; see <http://zlib.net>.
- [19] The *bzip2* utilities comprise a general purpose data-compression library. Here we used *bzip2* version 1.0.3; see <http://bzip.org>.
- [20] The *lzma* utilities comprise a general purpose data-compression library, which, in practice, is reported to yield a high compression ratio. Here we used the python module *pylzma* 0.4.4 as a wrapper to the *lzma* software development kit; see <https://pypi.python.org/pypi/pylzma>.
- [21] C. R. Shalizi and J. P. Crutchfield, *J. Stat. Phys.* **104**, 817 (2001).
- [22] D. Loewenstern, H. Hirsh, P. Yianilos, and M. Noordewier, DIMACS Technical Report No. 95-04, DIMACS Center-Rutgers University, 1977.
- [23] A. Baronchelli, E. Caglioti, and V. Loreto, *Eur. J. Phys.* **26**, S69 (2005).
- [24] P. Grassberger, [arXiv:physics/0207023](https://arxiv.org/abs/physics/0207023).
- [25] D. Benedetto, E. Caglioti, and V. Loreto, *Phys. Rev. Lett.* **88**, 048702 (2002).
- [26] D. V. Khmelev and W. J. Teahan, *Phys. Rev. Lett.* **90**, 089803 (2003).
- [27] J. Goodman, [arXiv:cond-mat/0202383](https://arxiv.org/abs/cond-mat/0202383).
- [28] A. Lesne, J.-L. Blanc, and L. Pezard, *Phys. Rev. E* **79**, 046208 (2009).
- [29] L. Liu, D. Li, and F. Bai, *Chem. Phys. Lett.* **530**, 107 (2012).
- [30] M. E. J. Newman and G. T. Barkema, *Monte Carlo Methods in Statistical Physics* (Clarendon Press, Oxford, UK, 1999).
- [31] T. Schürmann and P. Grassberger, *Chaos* **6**, 414 (1996).
- [32] J. P. Crutchfield and K. Young, *Phys. Rev. Lett.* **63**, 105 (1989).
- [33] J. P. Crutchfield, D. P. Feldman, and C. R. Shalizi, *Phys. Rev. E* **62**, 2996 (2000).
- [34] J. S. Shiner, M. Davison, and P. T. Landsberg, *Phys. Rev. E* **59**, 1459 (1999).
- [35] P.-M. Binder and N. Perry, *Phys. Rev. E* **62**, 2998 (2000).
- [36] J. S. Shiner, M. Davison, and P. T. Landsberg, *Phys. Rev. E* **62**, 3000 (2000).
- [37] R. López-Ruiz, H. L. Mancini, and X. Calbet, *Phys. Lett. A* **209**, 321 (1995).
- [38] T. M. Cover and J. A. Thomas, *Elements of Information Theory* (Wiley, New York, 2006).
- [39] I. Erb and N. Ay, *J. Stat. Phys.* **115**, 949 (2004).
- [40] K. Lindgren, in *Cellular Automata and Modeling of Complex Physical Systems*, edited by P. Manneville, N. Boccara, G. Y. Vichniac, and R. Bidaux (Springer, Berlin, 1989), p. 67.
- [41] T. Helvik and K. Lindgren, *J. Stat. Phys.* **155**, 687 (2014).
- [42] H. W. Lau and P. Grassberger, *Phys. Rev. E* **87**, 022128 (2013).
- [43] M. A. Jimenez-Montano, W. Ebeling, T. Pohl, and P. E. Rapp, *BioSystems* **64**, 23 (2002).
- [44] A. K. Hartmann, *Practical Guide to Computer Simulations* (World Scientific, Singapore, 2009).
- [45] E. E. Vogel, G. Saravia, and L. V. Cortez, *Phys. A (Amsterdam, Neth.)* **391**, 1591 (2012).